

# Analysis for MHD flow of a Maxwell fluid past a vertical stretching sheet in the presence of thermophoresis and chemical reaction

Noor Fadiya Mohd Noor

**Abstract**—The hydromagnetic flow of a Maxwell fluid past a vertical stretching sheet with thermophoresis is considered. The impact of chemical reaction species to the flow is analyzed for the first time by using the homotopy analysis method (HAM). The  $\bar{h}$ -curves for the flow boundary layer equations are presented graphically. Several values of wall skin friction, heat and mass transfer are obtained and discussed.

**Keywords**—homotopy, MHD, thermophoresis, chemical reaction, Maxwell.

## I. INTRODUCTION

THE non-Newtonian fluids have not been successfully described due to non-existence of a single constitutive relationships between stress and rate of strain. Since there are many industrial applications based on non-Newtonian fluids with convective heat and mass transfer such as in material processing, crystal growing, cooling of nuclear reactors, movement of biological fluids and other practical situations, the research on non-Newtonian fluids have become a great interest. Among the several models of non-Newtonian fluids that have been examined include the simplest subclass fluids known as Maxwell model.

Fatecau and Fatecau solved the Rayleigh-Stokes problem [1] and the Maxwell fluid flow past an infinite plate [2]. Sadeghy et al. [3] did a comparative study for Sakiadis flow of an upper-convected Maxwell (UCM) fluid on a rigid plate and concluded that the wall skin friction decreases with an increase in Deborah number. Hayat and Sajid [4] provided the series solution for MHD boundary layer flow of a UCM fluid by using the homotopy method while Wang and Hayat [5] investigated two-dimensional flow of an incompressible viscoelastic Maxwell fluid past an infinite porous plate. Other research on Maxwell fluid flow include the unsteady flow of a generalized Maxwell fluid with fractional derivative by Fatecau et al. [6], the effects of chemical reaction species [7], the mass transfer of a UCM fluid flow [8] and the radiation effects on MHD flow in a channel with porous medium [9].

In this paper, the study of MHD flow of a Maxwell fluid with thermophoresis previously considered by Hayat and Qasim [10] will be extended to include the effect of chemical reaction species for the first time by using the homotopy analysis method (HAM). This method first developed by Liao [11] has been successfully applied to many fluid flow and

heat transfer problems, cf. [12]–[16]. Noor et al. [17] have presented the homotopy solutions for thin film flow on an unsteady stretching sheet where a general surface temperature has been introduced. This work has been extended by Noor and Hashim [18] to determine the magnetic and thermocapillary effects in the thin film flow.

## II. PROBLEM FORMULATION

### A. Governing equations and boundary conditions

Consider a steady MHD flow of a Maxwell fluid past a vertical stretching sheet in a Darcian porous medium. A uniform magnetic field  $B_0$  is applied normal to the flow. The magnetic Reynolds number is sufficiently small such that the induced magnetic field can be neglected. The surface has variable temperature  $T_w(x)$  and variable concentration  $C_w(x)$  while the fluid has uniform ambient temperature  $T_\infty$  and uniform ambient concentration  $C_\infty$  where  $T_w > T_\infty$  and  $C_w > C_\infty$  respectively. Under these assumptions and Boussineq's approximation, the governing equations for the boundary layer flow are written as

$$\frac{\partial u}{\partial x} + \frac{\partial v}{\partial y} = 0, \quad (1)$$

$$u \frac{\partial u}{\partial x} + v \frac{\partial u}{\partial y} + \lambda_1 \left[ u^2 \frac{\partial^2 u}{\partial x^2} + v^2 \frac{\partial^2 u}{\partial y^2} + 2uv \frac{\partial^2 u}{\partial x \partial y} \right] = \nu \frac{\partial^2 u}{\partial y^2} - \frac{\nu}{K} u - \frac{\sigma B_0^2}{\rho} \left( u + \lambda_1 v \frac{\partial u}{\partial y} \right) + g[\beta_T(T - T_\infty) + \beta_C(C - C_\infty)], \quad (2)$$

$$u \frac{\partial T}{\partial x} + v \frac{\partial T}{\partial y} = \frac{\lambda_g}{\rho c_p} \frac{\partial^2 T}{\partial y^2} - \frac{1}{\rho c_p} \frac{\partial q_r}{\partial y} + \frac{\mu}{\rho c_p} \left( \frac{\partial u}{\partial y} \right)^2 + \frac{\sigma B_0^2}{\rho c_p} u^2, \quad (3)$$

$$u \frac{\partial C}{\partial x} + v \frac{\partial C}{\partial y} = D \frac{\partial^2 C}{\partial y^2} - \frac{\partial(V_T C)}{\partial y} - k_2 C, \quad (4)$$

subject to the boundary conditions

$$u = U_w(x) = ax, \quad v = 0, \quad T = T_w(x) = T_\infty + bx, \\ C = C_w(x) = C_\infty + cx \quad \text{at } y = 0, \quad (5)$$

$$u \rightarrow 0, \quad \frac{\partial u}{\partial y} \rightarrow 0, \quad T \rightarrow T_\infty, \quad C \rightarrow C_\infty, \\ \text{as } y \rightarrow \infty, \quad (6)$$

where  $u$  and  $v$  are the velocity components in the  $x, y$  directions,  $\nu$  is the kinematic viscosity,  $\rho$  is the fluid density,

$K$  is the permeability of porous medium,  $\sigma$  is the electrical conductivity,  $g$  is the acceleration due to gravity,  $T$  is the fluid temperature,  $C$  is the concentration field,  $\beta_T, \beta_C$  are the thermal expansion coefficients of temperature and concentration respectively,  $\lambda_g$  is the fluid thermal conductivity,  $c_p$  is the specific heat at constant pressure,  $q_r$  is the radiative heat flux in the  $y$ -direction,  $\mu$  is the dynamic viscosity,  $D$  is the molecular diffusivity of the species concentration,  $V_T$  is the thermophoretic velocity and  $k_2$  is the chemical reaction parameter.

The radiative heat flux  $q_r$  under Rosseland approximation has the form

$$q_r = -\frac{4\sigma_1}{3k^*} \frac{\partial T^4}{\partial y}, \quad (7)$$

where  $\sigma_1$  is the Stefan-Boltzmann constant and  $k^*$  is the mean absorption coefficient.

The temperature differences within the flow are assumed to be sufficiently small such that  $T^4$  may be expressed as a linear function of temperature. Expanding  $T^4$  using Taylor series and neglecting higher order terms yields

$$T^4 \cong 4T_\infty^3 T - 3T_\infty^4. \quad (8)$$

Using equations (7) and (8), we have

$$u \frac{\partial T}{\partial x} + v \frac{\partial T}{\partial y} = \frac{\lambda_g}{\rho c_p} \frac{\partial^2 T}{\partial y^2} + \frac{16\sigma_1 T_\infty^3}{3\rho c_p k^*} \frac{\partial^2 T}{\partial y^2} + \frac{\mu}{\rho c_p} \left( \frac{\partial u}{\partial y} \right)^2 + \frac{\sigma B_0^2(x)}{\rho c_p} u^2. \quad (9)$$

The second, third, fourth and fifth terms on the RHS of the equation (9) denote the thermal radiation, viscous and magnetic heating terms respectively.

Now the thermophoretic velocity  $V_T$  which appears in the equation (4) can be written as:

$$V_T = -k\nu \frac{\nabla T}{T_r} = -\frac{k\nu}{T_r} \frac{\partial T}{\partial y}, \quad (10)$$

where  $T_r$  is a reference temperature and  $k$  is the thermophoretic coefficient with range of value from 0.2 to 1.2. A thermophoretic parameter  $\tau$  can now be defined as:

$$\tau = -\frac{k(T_w - T_\infty)}{T_r}. \quad (11)$$

### B. Similarity transformation

The governing equations (2)–(4) can be transformed to a set of nonlinear ordinary differential equations by introducing the following non-dimensional variables:

$$\eta = \sqrt{\frac{a}{\nu}} y, \quad \psi = \sqrt{a\nu} x f(\eta),$$

$$\theta(\eta) = \frac{T - T_\infty}{T_w - T_\infty}, \quad \phi(\eta) = \frac{C - C_\infty}{C_w - C_\infty}, \quad (12)$$

where  $\psi$  is the stream function that satisfies the continuity equation (1) with

$$u = \frac{\partial \psi}{\partial y} = a x f'(\eta), \quad v = -\frac{\partial \psi}{\partial x} = -\sqrt{a\nu} f(\eta). \quad (13)$$

Using (12) and (13), the following similarity equations with the corresponding boundary conditions are obtained:

$$f''' + (1 + M\beta)f f'' - (f')^2 + \beta[2ff'f'' - f^2 f'''] - (\lambda + M)f' + \gamma[\theta + N\phi] = 0, \quad (14)$$

$$\left(1 + \frac{4}{3}R_d\right)\theta'' + \text{Pr}(f\theta' - f'\theta) + \text{Pr}Ec(Mf'^2 + f''^2) = 0, \quad (15)$$

$$\phi'' + Sc[f\phi' - f'\phi - \tau(\theta'\phi' + \theta''\phi)] - K_2\phi = 0, \quad (16)$$

subject to

$$f(0) = 0, \quad f'(0) = 1, \quad \theta(0) = 1, \quad \phi(0) = 1, \quad \text{at } \eta = 0, \quad (17)$$

$$f' \rightarrow 0, \quad f'' \rightarrow 0, \quad \theta \rightarrow 0, \quad \phi \rightarrow 0, \quad \text{as } \eta \rightarrow \infty, \quad (18)$$

where  $\beta = \lambda_1 a$  is the Deborah number,  $M = \sigma B_0^2 / \rho a$  is the Hartmann number,  $\lambda = \nu / aK$  is the porosity parameter,  $\gamma = Gr_x / Re_x^2$  is the local buoyancy parameter,  $Gr_x = g\beta_T(T_w - T_\infty)x^3 / \nu^2$  is the Grashof number,  $Re_x = u_w x / \nu$  is the Reynolds number,  $N = \beta_C(C_w - C_\infty) / (\beta_T(T_w - T_\infty))$ ,  $Rd = 4\sigma_1 T_\infty^3 / k^* \lambda_g$ ,  $\text{Pr}$  is the Prandtl number,  $Ec = u_w^2 / (c_p(T_w - T_\infty))$  is the Eckert number,  $Sc = \nu / D$  is the Schmidt number and  $K_2 = k_2 Sc / a$  is the chemical reaction parameter.

### III. HAM SOLUTION

The velocity  $f(\eta)$ , temperature  $\theta(\eta)$  and the concentration  $\phi(\eta)$  fields can be expressed by the set of base functions  $\{\eta^i \exp(-n\eta) | i, n \geq 0\}$  as follows [10]

$$f(\eta) = a_{0,0} + \sum_{n=0}^{\infty} \sum_{i=0}^{\infty} a_{n,i} \eta^i e^{-n\eta}, \quad (19)$$

$$\theta(\eta) = \sum_{n=0}^{\infty} \sum_{i=0}^{\infty} b_{n,i} \eta^i e^{-n\eta}, \quad (20)$$

$$\phi(\eta) = \sum_{n=0}^{\infty} \sum_{i=0}^{\infty} c_{n,i} \eta^i e^{-n\eta}, \quad (21)$$

where  $a_{n,i}$ ,  $b_{n,i}$  and  $c_{n,i}$  are the coefficients. The initial guesses  $f_0, \theta_0$  and  $\phi_0$  of  $f(\eta), \theta(\eta)$  and  $\phi(\eta)$  based on the rule of solution expressions and the boundary conditions are

$$f_0(\eta) = 1 - e^{-\eta}, \quad (22)$$

$$\theta_0(\eta) = e^{-\eta}, \quad (23)$$

$$\phi_0(\eta) = e^{-\eta}. \quad (24)$$

The following auxiliary linear operators

$$\mathcal{L}_f = \frac{\partial^3 f}{\partial \eta^3} - \frac{\partial f}{\partial \eta}, \quad (25)$$

$$\mathcal{L}_\theta = \frac{\partial^2 \theta}{\partial \eta^2} - \theta, \quad (26)$$

$$\mathcal{L}_\phi = \frac{\partial^2 \phi}{\partial \eta^2} - \phi. \quad (27)$$

are chosen with the properties

$$\mathcal{L}_f[C_1 + C_2e^\eta + C_3e^{-\eta}] = 0, \quad (28)$$

$$\mathcal{L}_\theta[C_4e^\eta + C_5e^{-\eta}] = 0, \quad (29)$$

$$\mathcal{L}_\phi[C_6e^\eta + C_7e^{-\eta}] = 0, \quad (30)$$

where  $C_i, (i = 1, \dots, 7)$  are the arbitrary constants.

If  $q \in [0, 1]$  is the embedding parameter,  $\hbar_f, \hbar_\theta$  and  $\hbar_\phi$  are the nonzero auxiliary parameters whereas  $H_f, H_\theta$  and  $H_\phi$  are nonzero auxiliary functions respectively, then the zeroth order deformation equations can be constructed as

$$(1 - q)\mathcal{L}_f[F(\eta; q) - f_0(\eta)] = q\hbar_f H_f \mathcal{N}_f[F(\eta; q), \Theta(\eta; q), \Phi(\eta; q)], \quad (31)$$

$$(1 - q)\mathcal{L}_\theta[\Theta(\eta; q) - \theta_0(\eta)] = q\hbar_\theta H_\theta \mathcal{N}_\theta[F(\eta; q), \Theta(\eta; q), \Phi(\eta; q)], \quad (32)$$

$$(1 - q)\mathcal{L}_\phi[\Phi(\eta; q) - \phi_0(\eta)] = q\hbar_\phi H_\phi \mathcal{N}_\phi[F(\eta; q), \Theta(\eta; q), \Phi(\eta; q)], \quad (33)$$

subject to

$$\begin{aligned} F(0; q) = 0, \quad F'(\infty; q) = 0, \\ \Theta(0; q) = 1, \quad \Theta(\infty; q) = 0, \\ \Phi(0; q) = 1, \quad \Phi(\infty; q) = 0, \end{aligned} \quad (34)$$

where the nonlinear operators  $\mathcal{N}_f, \mathcal{N}_\theta$  and  $\mathcal{N}_\phi$  are

$$\begin{aligned} \mathcal{N}_f[F(\eta; q), \Theta(\eta; q), \Phi(\eta; q)] = & F'''(\eta; q) + (1 + M\beta)F(\eta; q)F'''(\eta; q) \\ & - [F'(\eta; q)]^2 - (\lambda + M)F'(\eta; q) \\ & + 2\beta F(\eta; q)F'(\eta; q)F''(\eta; q) - \beta[F(\eta; q)]^2 F'''(\eta; q) \\ & + \gamma[\Theta(\eta; q) + N\Phi(\eta; q)], \end{aligned} \quad (35)$$

$$\begin{aligned} \mathcal{N}_\theta[F(\eta; q), \Theta(\eta; q), \Phi(\eta; q)] = & \left(1 + \frac{4}{3}Rd\right)\Theta''(\eta; q) + \text{Pr}[F(\eta; q)\Theta'(\eta; q) \\ & - F'(\eta; q)\Theta(\eta; q)] + \text{Pr}Ec[F''(\eta; q)]^2 \\ & + \text{Pr}EcM[F'(\eta; q)]^2, \end{aligned} \quad (36)$$

$$\begin{aligned} \mathcal{N}_\phi[F(\eta; q), \Theta(\eta; q), \Phi(\eta; q)] = & \Phi''(\eta; q) + Sc[F(\eta; q)\Phi'(\eta; q) - F'(\eta; q)\Phi(\eta; q)] \\ & - Sc\tau[\Theta'(\eta; q)\Phi'(\eta; q) + \Theta''(\eta; q)\Phi(\eta; q)] \\ & - K_2\Phi(\eta; q). \end{aligned} \quad (37)$$

When  $q = 0$  and  $q = 1$ , we have

$$\begin{aligned} F(\eta; 0) = f_0(\eta), \quad F(\eta; 1) = f(\eta), \\ \Theta(\eta; 0) = \theta_0(\eta), \quad \Theta(\eta; 1) = \theta(\eta), \\ \Phi(\eta; 0) = \phi_0(\eta), \quad \Phi(\eta; 1) = \phi(\eta). \end{aligned} \quad (38)$$

By Taylor series and using (38),  $F(\eta; q), \Theta(\eta; q)$  and  $\Phi(\eta; q)$  can be expanded as series of  $q$ ,

$$\begin{aligned} F(\eta; q) = f_0(\eta) + \sum_{m=1}^{+\infty} f_m(\eta)q^m, \\ \Theta(\eta; q) = \theta_0(\eta) + \sum_{m=1}^{+\infty} \theta_m(\eta)q^m, \\ \Phi(\eta; q) = \phi_0(\eta) + \sum_{m=1}^{+\infty} \phi_m(\eta)q^m, \end{aligned} \quad (39)$$

where

$$\begin{aligned} f_m(\eta) = \frac{1}{m!} \left[ \frac{\partial^m F(\eta; q)}{\partial q^m} \right]_{q=0}, \\ \theta_m(\eta) = \frac{1}{m!} \left[ \frac{\partial^m \Theta(\eta; q)}{\partial q^m} \right]_{q=0}, \\ \phi_m(\eta) = \frac{1}{m!} \left[ \frac{\partial^m \Phi(\eta; q)}{\partial q^m} \right]_{q=0}. \end{aligned} \quad (40)$$

The auxiliary parameters and functions are properly chosen so that the deformation equations (31)–(33) converge at  $q = 1$ . Hence

$$f(\eta) = f_0(\eta) + \sum_{m=1}^{+\infty} f_m(\eta), \quad (41)$$

$$\theta(\eta) = \theta_0(\eta) + \sum_{m=1}^{+\infty} \theta_m(\eta), \quad (42)$$

$$\phi(\eta) = \phi_0(\eta) + \sum_{m=1}^{+\infty} \phi_m(\eta). \quad (43)$$

The  $m$ th-order deformation equations are obtained as follows

$$\mathcal{L}_f[f_m(\eta) - \chi_m f_{m-1}(\eta)] = \hbar_f H_f(\eta) \mathcal{R}_m^f(\eta), \quad (44)$$

$$\mathcal{L}_\theta[\theta_m(\eta) - \chi_m \theta_{m-1}(\eta)] = \hbar_\theta H_\theta(\eta) \mathcal{R}_m^\theta(\eta), \quad (45)$$

$$\mathcal{L}_\phi[\phi_m(\eta) - \chi_m \phi_{m-1}(\eta)] = \hbar_\phi H_\phi(\eta) \mathcal{R}_m^\phi(\eta), \quad (46)$$

subject to the boundary conditions

$$\begin{aligned} f_m(0) = 0, \quad f'_m(0) = 0, \quad \theta_m(0) = 0, \quad \phi_m(0) = 0, \\ f'_m(\infty) = 0, \quad \theta_m(\infty) = 0, \quad \phi_m(\infty) = 0, \end{aligned} \quad (47)$$

for  $m \geq 1$ , where

$$\begin{aligned} \mathcal{R}_m^f(\eta) = & f'''_{m-1} - (\lambda + M)f'_{m-1} \\ & + \sum_{i=0}^{m-1} [(1 + M\beta)f_i f''_{m-1-i} - f'_i f'_{m-1-i}] \\ & + 2\beta \sum_{i=0}^{m-1} \sum_{l=0}^i f_l f'_{i-l} f''_{m-1-i} - \beta \sum_{i=0}^{m-1} \sum_{l=0}^i f_l f_{i-l} f'''_{m-1-i} \\ & + \gamma(\theta_{m-1} + N\phi_{m-1}), \end{aligned} \quad (48)$$

$$\begin{aligned} \mathcal{R}_m^\theta(\eta) = & \left(1 + \frac{4}{3}Rd\right)\theta''_{m-1} \\ & + \text{Pr} \sum_{i=0}^{m-1} [f_i \theta'_{m-1-i} - f'_{m-1-i} \theta_i] \\ & + \text{Pr}Ec \sum_{i=0}^{m-1} [M f'_i f'_{m-1-i} + f''_i f''_{m-1-i}], \end{aligned} \quad (49)$$

$$\begin{aligned} \mathcal{R}_m^\phi(\eta) = & \phi''_{m-1} + Sc \sum_{i=0}^{m-1} [f_i \phi'_{m-1-i} - f'_{m-1-i} \phi_i] \\ & - Sc\tau \sum_{i=0}^{m-1} [\theta'_i \phi'_{m-1-i} + \theta''_{m-1-i} \phi_i] - K_2 \phi_{m-1}, \end{aligned} \quad (50)$$

and

$$\chi_m = \begin{cases} 1, & m > 1, \\ 0, & m = 1. \end{cases}$$

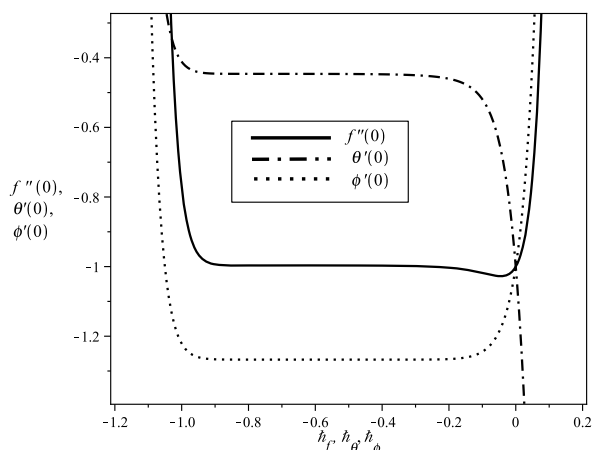


Fig. 1.  $\hbar$ -curves of  $f''(0)$ ,  $\theta'(0)$  and  $\phi'(0)$  at 25th HAM order of approximation when  $\beta = \tau = 0.2$ ,  $N = K_2 = M = \lambda = \gamma = 1.0$ ,  $Ec = Sc = 0.5$ ,  $R_d = 0.3$  and  $Pr = 0.7$ .

TABLE I  
 CONVERGENCE OF HAM SOLUTIONS AT DIFFERENT ORDER OF APPROXIMATIONS WHEN  $\hbar_f = \hbar_\theta = \hbar_\phi = -0.6$ ,  $\beta = \tau = 0.2$ ,  $N = K_2 = M = \lambda = \gamma = 1.0$ ,  $Ec = Sc = 0.5$ ,  $R_d = 0.3$  AND  $Pr = 0.7$ .

HAM order	$-f''(0)$	$-\theta'(0)$	$-\phi'(0)$
1	1.05000	0.65000	1.19000
5	1.00541	0.46368	1.26632
10	0.99802	0.44908	1.26728
15	0.99688	0.44681	1.26728
20	0.99665	0.44634	1.26728
25	0.99660	0.44624	1.26728
30	0.99659	0.44622	1.26728
35	0.99659	0.44622	1.26728

#### IV. RESULTS AND DISCUSSION

The auxiliary functions  $H_f(\eta)$ ,  $H_\theta(\eta)$  and  $H_\phi(\eta)$  are set to be equal to 1 in all calculations done in this paper. The convergence of HAM solutions now rely on the selection of values of the auxiliary parameters  $\hbar_f$ ,  $\hbar_\theta$  and  $\hbar_\phi$ . The  $\hbar$  curves at 25th order of HAM approximation when  $N = K_2 = M = \lambda = \gamma = 1.0$ ,  $Ec = Sc = 0.5$ ,  $R_d = 0.3$  and  $Pr = 0.7$  are presented in Fig. 1 for this purpose. Based on this figure, the convergent solutions for  $f''(0)$ ,  $\theta'(0)$  and  $\phi'(0)$  can be obtained in the range of  $-0.9 < \hbar_f < -0.4$ ,  $-0.9 < \hbar_\theta < -0.5$  and  $-0.9 < \hbar_\phi < -0.2$ . For simplicity, the value of  $\hbar_f = \hbar_\theta = \hbar_\phi = -0.6$  is used throughout this paper. The convergence of the homotopy analysis solutions up to the 35th order of approximation can be observed as in Table I.

The effects of thermophoresis, Hartmann number, porosity, chemical reaction and Schmidt number on wall skin friction, heat flux and mass flux are revealed in Table II–VI respectively. As defined previously in the initial/boundary conditions (17)–(18), the velocity, temperature and concentration distributions decay as  $\eta$  tends to infinity. Based on Table II, it can be concluded that as the Hartmann number increases, the Lorentz drag force due to electromagnetism increases leading to increment in the skin friction. Thus the thickness of the velocity boundary layer decreases as well as the velocity rundown. With higher value of wall skin friction  $-f''(0)$ , more heat is absorbed which results in less heat flux  $-\theta'(0)$

TABLE II  
 EFFECTS OF HARTMANN NUMBER ON THE SKIN FRICTION, HEAT FLUX AND MASS FLUX WHEN  $\hbar_f = \hbar_\theta = \hbar_\phi = -0.6$ ,  $\beta = \tau = 0.2$ ,  $N = K_2 = \lambda = \gamma = 1.0$ ,  $Ec = Sc = 0.5$ ,  $R_d = 0.3$  AND  $Pr = 0.7$ .

$M$	$-f''(0)$	$-\theta'(0)$	$-\phi'(0)$
0.0	0.61105	0.63589	1.30284
0.5	0.81242	0.53469	1.28395
1.0	0.99660	0.44624	1.26728
2.0	1.38934	0.28290	1.24527

TABLE III  
 EFFECTS OF POROSITY ON THE SKIN FRICTION, HEAT FLUX AND MASS FLUX WHEN  $\hbar_f = \hbar_\theta = \hbar_\phi = -0.6$ ,  $\beta = \tau = 0.2$ ,  $N = K_2 = M = \gamma = 1.0$ ,  $Ec = Sc = 0.5$ ,  $R_d = 0.3$  AND  $Pr = 0.7$ .

$\lambda$	$-f''(0)$	$-\theta'(0)$	$-\phi'(0)$
0.0	0.61270	0.50658	1.29285
0.5	0.81416	0.47655	1.27937
1.0	0.99660	0.44624	1.26728
2.0	1.34492	0.38715	1.24895

TABLE IV  
 EFFECTS OF THERMOPHORESIS ON THE SKIN FRICTION, HEAT FLUX AND MASS FLUX WHEN  $\hbar_f = \hbar_\theta = \hbar_\phi = -0.6$ ,  $\beta = \tau = 0.2$ ,  $N = K_2 = M = \lambda = \gamma = 1.0$ ,  $Ec = Sc = 0.5$ ,  $R_d = 0.3$  AND  $Pr = 0.7$ .

$\tau$	$-f''(0)$	$-\theta'(0)$	$-\phi'(0)$
0.0	0.99396	0.44709	1.24182
0.2	0.99660	0.44624	1.26728
0.5	1.00052	0.44499	1.30586
1.0	1.00695	0.44298	1.37122

TABLE V  
 EFFECTS OF CHEMICAL REACTION ON THE SKIN FRICTION, HEAT FLUX AND MASS FLUX WHEN  $\hbar_f = \hbar_\theta = \hbar_\phi = -0.6$ ,  $\beta = \tau = 0.2$ ,  $N = M = \lambda = \gamma = 1.0$ ,  $Ec = Sc = 0.5$ ,  $R_d = 0.3$  AND  $Pr = 0.7$ .

$K_2$	$-f''(0)$	$-\theta'(0)$	$-\phi'(0)$
0.0	0.92029	0.47847	0.70970
0.5	0.96935	0.45647	1.03512
1.0	0.99660	0.44624	1.26728
2.0	1.03073	0.43520	1.62744

from the surface. Consequently, the amount of mass deposited on the surface declines due to the nature of thermophoresis where small or nano particles tend to be driven away from the hot surface to cool surroundings. Imposing greater porosity on the vertical surface caused greater force in the opposite direction of the flow as listed in Table III. Thus the skin friction increases and the velocity declines. The same occurrences for  $-\theta'(0)$  and  $-\phi'(0)$  as the Hartmann number increases are expected with a positive change in the surface porosity due to addition to wall skin friction values.

The numerical results in Table IV–VI show consistent increments in the flow skin friction and mass flux but decrements in the flow heat flux as thermophoresis, chemical reaction and Schmidt number grow. Obviously, thermophoresis has direct impact on the concentration profile rather than on the flow velocity and temperature distributions as shown in Table IV. As the chemical reaction species in the flow are multiplied, higher fluid composition can be flushed away from the surface as given in Table V. Similar occurrence is observed in Table VI where the mass flux  $-\phi'(0)$  increases ( $\phi'(0)$  decreases) when Schmidt number, the ratio of momentum diffusivity towards mass diffusivity increases.

TABLE VI

EFFECTS OF SCHMIDT NUMBER ON THE SKIN FRICTION, HEAT FLUX AND MASS FLUX WHEN  $\tilde{h}_f = \tilde{h}_\theta = \tilde{h}_\phi = -0.6, \beta = \tau = 0.2, N = M = \lambda = \gamma = 1.0, Ec = 0.5, R_d = 0.3$  AND  $Pr = 0.7$ .

$Sc$	$-f''(0)$	$-\theta'(0)$	$-\phi'(0)$
0.0	0.96416	0.45873	1.00000
0.5	0.99660	0.44624	1.26728
1.0	1.02217	0.43747	1.50958
2.0	1.05972	0.42646	1.93913

## V. CONCLUSION

The steady boundary layer of a Maxwell fluid past a vertical stretching sheet in a Darcian porous medium with chemical reaction has been studied for the first time. In order to get the convergent solutions of HAM, the values for  $\tilde{h}_f, \tilde{h}_\theta$  and  $\tilde{h}_\phi$  have to be chosen properly between -0.9 and -0.2. The changes in the velocity, heat transfer as well as the mass transfer in the flow have been observed as Harmann number, porosity, thermophoresis, chemical reaction and Schmidt number vary. Clearly, as the values of thermophoresis, chemical reaction parameter and Schmidt number escalate, the thickness of the mass boundary layer declines.

## ACKNOWLEDGMENT

Financial support received under the grant FRGS/2/2010/SG/UNISEL/03/1 is greatly appreciated.

## REFERENCES

- [1] C. Fetecau and C. Fetecau, *The RayleighStokes-problem for a fluid of Maxwellian type*, International Journal of Non-Linear Mechanics, 38 (2003) 603607.
- [2] C. Fetecau and C. Fetecau, *An exact solution for the flow of a Maxwell fluid past an infinite plate*, International Journal of Non-Linear Mechanics, 38 (2003) 423-427.
- [3] K. Sadeghy, A.H. Najafi and M.Saffaripour, *Sakiadis flow of an upper-convected Maxwell fluid*, International Journal of Non-Linear Mechanics, 40 (2005) 1220-1228.
- [4] T. Hayat and M. Sajid, *Homotopy analysis of MHD boundary layer flow of an upper-convected Maxwell fluid*, International Journal of Engineering Science, 45 (2007) 393-401.
- [5] Y. Wang and T. Hayat, *Fluctuating flow of a Maxwell fluid past a porous plate with variable suction*, Nonlinear Analysis: Real World Applications, 9 (2008) 1269-1282.
- [6] C. Fetecau, M. Athar and C. Fetecau, *Unsteady flow of a generalized Maxwell fluid with fractional derivative due to a constantly accelerating plate*, Computers and Mathematics with Applications 57 (2009) 596-603.
- [7] T. Hayat, Z. Abbas and N. Alib, *MHD flow and mass transfer of a upper-convected Maxwell fluid past a porous shrinking sheet with chemical reaction species*, Physics Letters A 372 (2008) 4698-4704.
- [8] T. Hayat, M. Awais, M. Qasim and A.A. Hendi, *Effects of mass transfer on the stagnation point flow of an upper-convected Maxwell (UCM) fluid*, International Journal of Heat and Mass Transfer 54 (2011) 3777-3782.
- [9] T. Hayat, R. Sajjad, Z. Abbas, M. Sajid and A.A. Hendi, *Radiation effects on MHD flow of Maxwell fluid in a channel with porous medium*, International Journal of Heat and Mass Transfer 54 (2011) 854-862.
- [10] T. Hayat and M. Qasim, *Influence of thermal radiation and Joule heating on MHD flow of a Maxwell fluid in the presence of thermophoresis*, International Journal of Heat and Mass Transfer 53 (2010) 4780-4788.
- [11] S.J. Liao, *Beyond Perturbation: Introduction to the Homotopy Analysis Metho*, Chapman and Hall, Boca Raton (2003).
- [12] S.J. Liao and I. Pop, *Explicit analytic solution for similarity boundary layer equations*, International Journal of Heat and Mass Transfer 47 (2004) 75-78.
- [13] S.J. Liao, *A new branch of solutions of boundary-layer flows over an impermeable stretched plate*, International Journal of Heat and Mass Transfer, 48 (2005) 2529-3259.

- [14] H. Xu and S.J. Liao, *A series solution of the unsteady Von Karman swirling viscous flows*, Acta Applicandae Mathematicae 94 (2006) 215-231.
- [15] Z. Ziabakhsh and G. Domairry, *Analytic solution of natural convection flow of a non-Newtonian fluid between two vertical flat plates using homotopy analysis method*, Communication in Nonlinear Science and Numerical Simulation 14 (2009) 1868-1880.
- [16] O. Abdulaziz, N.F.M. Noor and I. Hashim, *Homotopy analysis method for fully developed MHD micropolar fluid flow between vertical porous plates*, International Journal for Numerical Methods in Engineering 78 (2009) 817-827.
- [17] N.F.M. Noor, O. Abdulaziz and I. Hashim, *MHD flow and heat transfer in a thin liquid film on an unsteady stretching sheet by the homotopy analysis method*, International Journal for Numerical Methods in Fluids 63 (2010) 357-373.
- [18] N.F.M. Noor and I. Hashim, *Thermocapillarity and magnetic field effects in a thin liquid film on an unsteady stretching surface*, International Journal of Heat and Mass Transfer 53 (2010) 2044-2051.

**Noor Fadiya Mohd Noor** born in 1981. She is among the first Malaysian researcher who applied analytical solutions via homotopy analysis method proposed by S. J. Liao (2003). Holding science bachelor and master degrees in mathematics from Universiti Teknologi Malaysia, she attained her Ph.D. from Universiti Kebangsaan Malaysia in 2010 under the supervision of Prof. Ishak Hashim. Passionate with analytical and numerical methods in fluid mechanics, she continue to study boundary layer model especially for viscous magnetohydrodynamic flows in her research. Published 10 articles in indexed journals and 4 articles in international conference proceedings so far, she is eager to learn and to reveal more analytical/numerical findings in the future. She also continuously seek opportunities to work with other researchers worldwide.